Inventory of Supplemental Information for Fuccillo et al. 2015

1. SUPPLEMENTARY FIGURES:

Supplementary Figure 1. Reduced contamination index in single cells suggests decreased inclusion of glial transcripts compared with tissue mRNA. Related to Figure 1, which describes our overall technical approach to single cell analysis.

Supplementary Figure 2. Tissue-specific expression profiles of synaptic adhesion molecules. Related to Figure 2/3, as it provides the rational for extending our analysis to the nucleus accumbens, a brain region with similar overall tissue splicing patterns as the hippocampus.

Supplementary Figure 3. Synaptic adhesion profiles of striatal circuits. Provides additional transcriptional profiling information for the three experimental paradigms exploring striatal circuits displayed in Figure 5.

Supplementary Figure 4. Synaptic adhesion molecule expression can predict neuronal cell type. Provides a summary of the clustering ability of different probe sets for Figures 2-6.

Supplementary Figure 5. Splice-site coordination between Nrxn1 and Nrxn3 is brain region-specific. Provides a complementary splice-site analysis to Figure 7, demonstrating coordinated regulation of splice sites across neurexin isoforms.

Supplementary Figure 6. Hypothetical functions for synaptic adhesion codes. Provides a graphical summary of the potential functions that a synaptic adhesion code could provide for circuit formation and plasticity (Figure 8).

2. SUPPLEMENTARY TABLES:

Supplementary Table S1. (provided as excel sheet) RT-PCR primer assays used to detect synaptic-adhesion molecule expression at the single cell level.

3. SUPPLEMENTAL EXTENDED EXPERIMENTAL PROCEDURES

4. SUPPLEMENTAL REFERENCES

Supplemental Information for Fuccillo et al. 2015
SUPPLEMENTARY FIGURES

A

$$Contamination\ Index\ (CI) = \frac{Single\ Cell^{CI}}{Tissue^{CI}} = \frac{\frac{SC^{Glial}}{SC^{Neuronal}}}{\frac{T^{Glial}}{T^{Neuronal}}}$$

SC=Single cell normalized expression
T=Tissue normalized expression
Glial Markers - Gfap, Slc1A2, Connexin30, Sox10
Neuronal Markers - Rbfox3, Nefl, Syt2, Syt1, Mapt

B

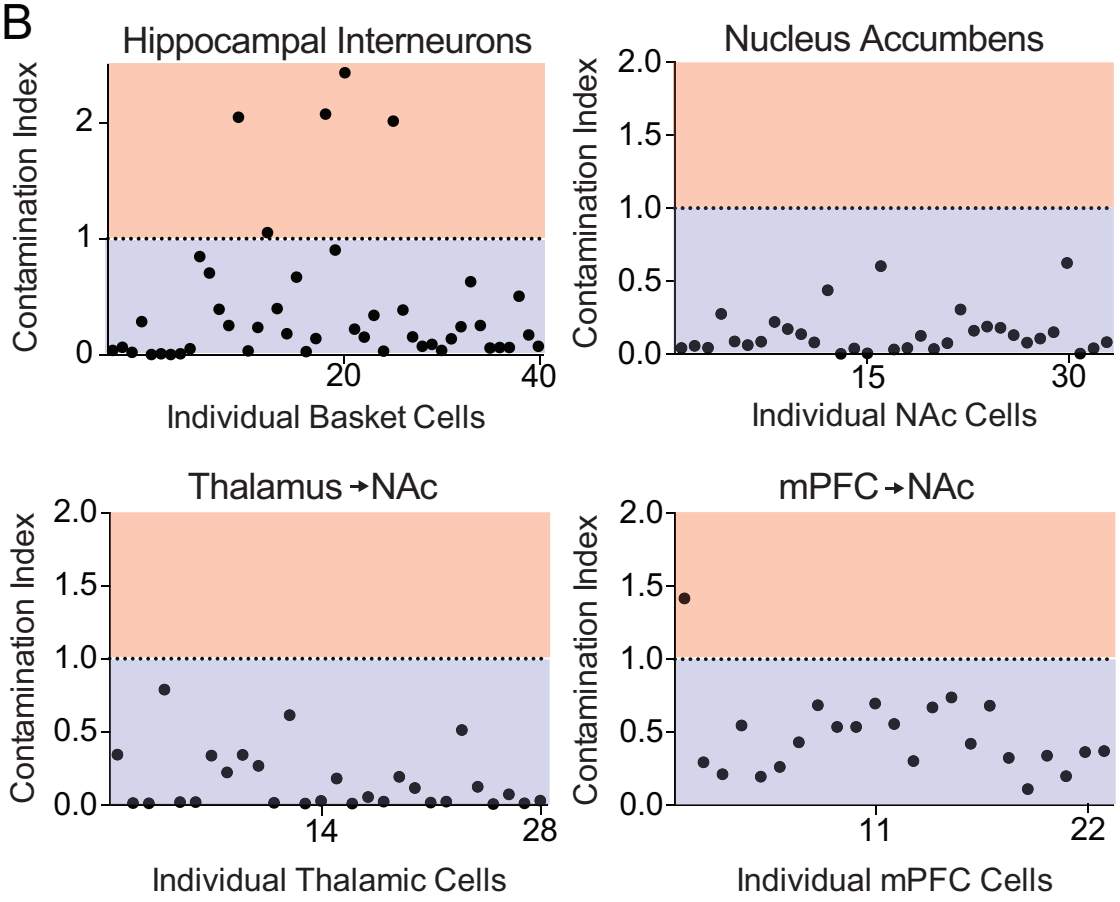

Supplementary Figure 1 (related to Figure 1). Reduced contamination index in single cells suggests decreased inclusion of glial transcripts compared with tissue mRNA.

(A) Formula for the calculation of the single cell contamination index. (B) The contamination index plotted for all cells in four of the major data sets analyzed. Contamination index of 1 (dotted line) indicates a similar level of glial marker expression in single cell samples as compared to tissue mRNA isolated from the same region.

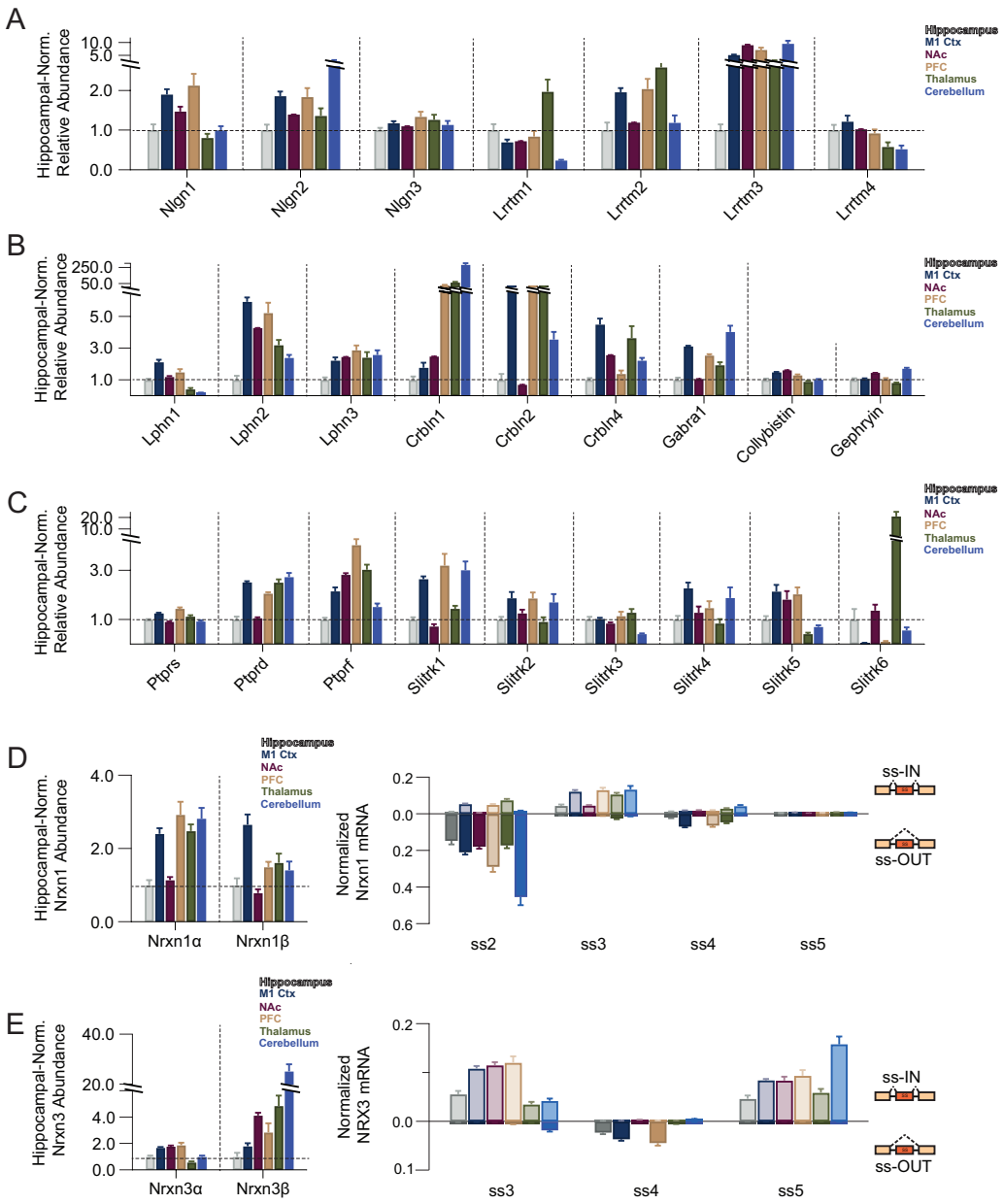

Supplementary Figure 2 (related to Figure 2). Tissue-specific expression profiles of synaptic adhesion molecules.

(A,B) Relative abundance of known neurexin ligands (and postsynaptic GABAergic molecules) in various tissues, normalized to hippocampal expression levels. (C) Relative abundance of Ptpr-s and their Slitrk ligands across various tissues, normalized to hippocampal expression levels. (D, left) Relative abundance of Nrxn1 across brain region, normalized to hippocampal levels. (D, right) Normalized expression of Nrxn1 splice-site specific probes across brain region, with SS-in and SS-out probes projecting upwards and downwards, respectively. (E, left) Relative abundance of Nrxn3 across brain region, normalized to hippocampal levels. (E, right) Normalized expression of Nrxn3 splice-site specific probes across brain region. All tissue data are means ± SEM of n=6 independent tissue samples.

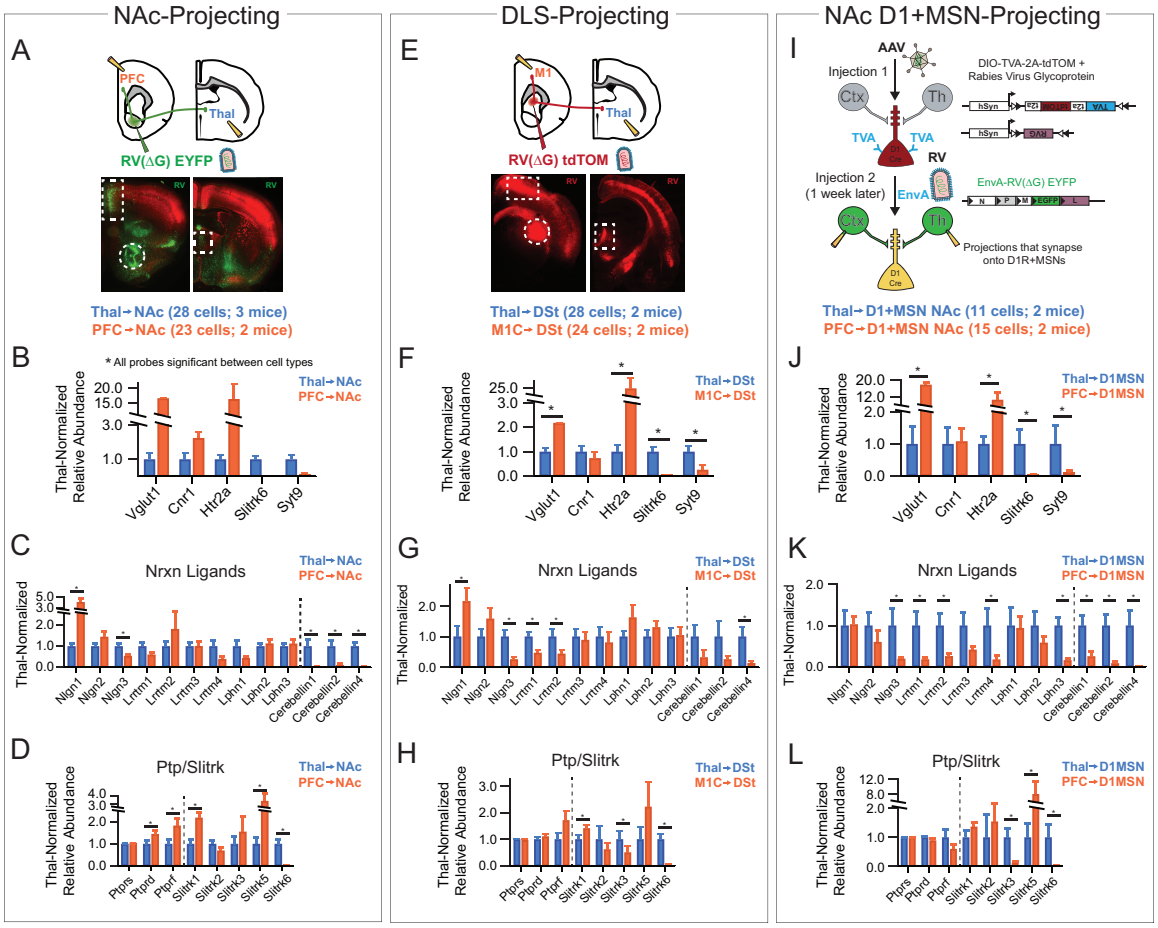

Supplementary Figure 3 (related to Figure 5). Synaptic adhesion profiles of striatal circuits.

Three RV-mediated retrograde tracing approaches to isolate cortical and thalamic inputs to the nucleus accumbens (A, n=28 thalamic cells, n=23 PFC cells), dorsolateral striatum (E, n=28 thalamic cells, n=24 M1 cells) and D1R+MSNs of the nucleus accumbens (I, n=11 thalamic cells, n=15 M1 cells). Thalamus-normalized relative mRNA abundance for marker probes (B,F,J), neurexin ligands (C,G,K) and Ptp/Slitrk molecules (D,H,L). Data are means ± SEM; *significant difference between groups (Mann Whitney U-test).

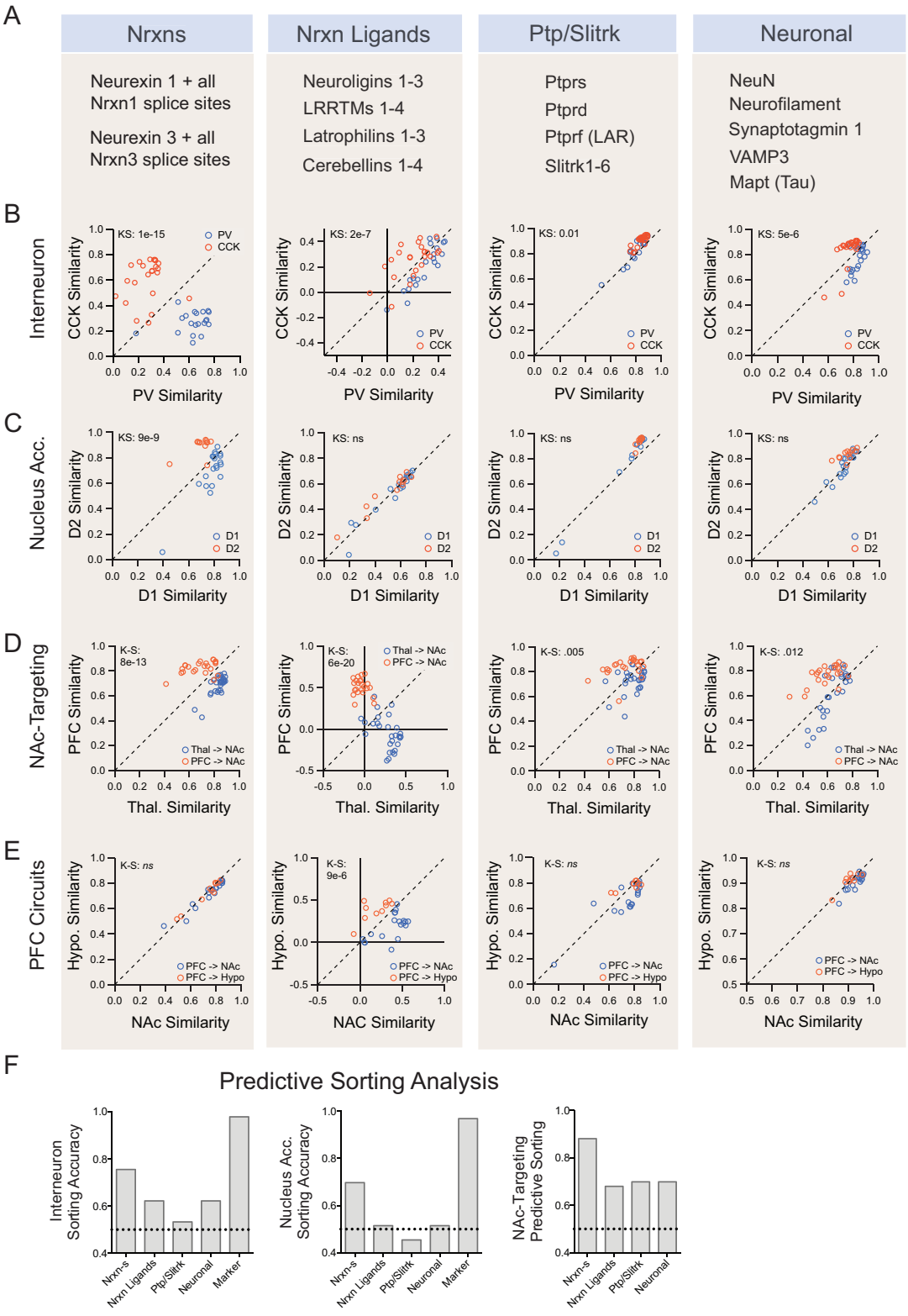

Supplementary Figure 4 (related to Figure 6). Synaptic adhesion molecule expression can predict neuronal cell type.

(A) Explanation of the probe sets used for the clustering analysis. (B-E) Plotting of single cell identity for interneurons (B, n=45 cells), NAc medium spiny neurons

(C, n=33 cells), NAc-targeting neurons (D, n=51 cells) and prefrontal cortex projection neurons (E, n=29 cells) as determined by Pearson's correlation coefficient-based clustering, according to probe sets for neurexins, neurexin ligands, ptprs/slitrk molecules and general neuronal probes (columns from left to right). (F) Accuracy of hierarchical sorting analysis, which divided single cells into two populations based on the probe sets in A (the additional "Marker" group comprises probes already known to distinguish cell types) for interneurons (left), NAc medium spiny neurons (middle) and NAc-projecting neuron (right) datasets. Dotted line at 0.5 signifies poor predictive power. Kolmogorov-Smirnov (KS) values are given for comparison of single cell groups in B-E.

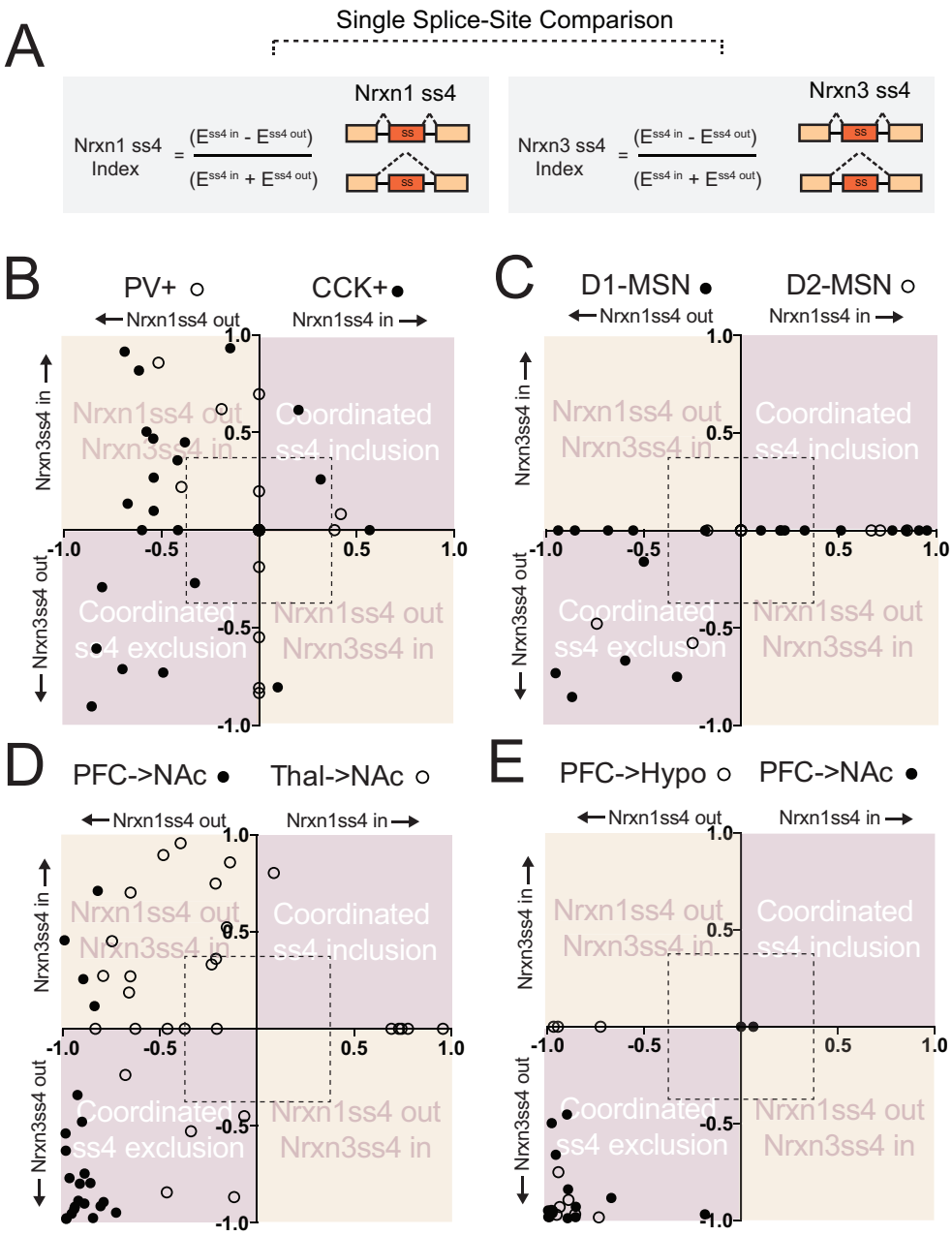

Supplementary Figure 5 (related to Figure 7). Splice-site coordination between Nrxn1 and Nrxn3 is brain region-specific.

(A) Description of Nrxn1 and Nrxn3 splice-site 4 indices, which assess exclusive presence of single splice isoforms or coexpression of ss4-IN and ss4-OUT transcripts. (B-E) Plot of Nrxn1 splice-site 4 index versus Nrxn3 splice-site 4 index for all single neurons collected in hippocampal interneuron (B, n=45 cells), NAc MSN (C, n=33 cells), NAc-projecting (D, n=51 cells) and divergent PFC projection (E, n=29 cells) experiments. Points falling within the hatched box surrounding the ordinate exhibit coexpressed ss4-IN and ss4-OUT for both neurexin1 and neurexin3.

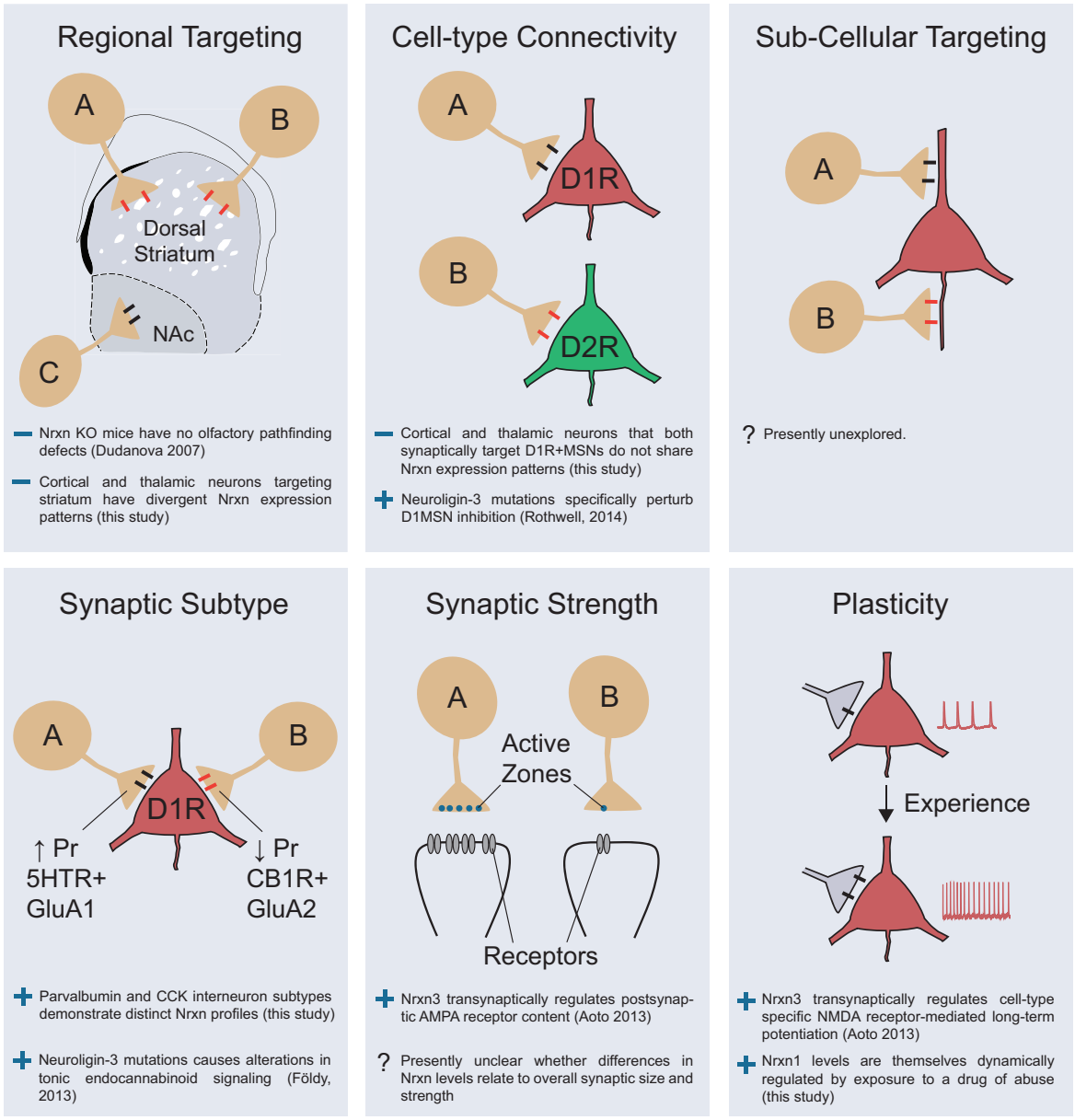

Supplementary Figure 6 (related to Figure 8). Hypothetical functions for synaptic adhesion codes.

Schematized putative functions for synaptic adhesion molecules including existing supporting (+) and inconsistent (-) evidence to date, as well as unexplored areas of study (?).

SUPPLEMENTARY TABLES

Attached as excel file

Table S1 (related to Figure 1). RT-PCR primer assays used to detect synaptic-adhesion molecule expression at the single-cell level.

Sequences for the forward primer, internal probe and reverse primer for all custom-designed Primetime assays used in our single-cell analysis. Blank fields are displayed for pre-designed q-PCR assays purchased from IDT.

SUPPLEMENTAL EXTENDED EXPERIMENTAL PROCEDURES

Animals

Generation of the PV-Cre (Hippenmeyer et al., 2007), D1-tomato (Shuen et al., 2008), D1-Cre (Gong et al., 2007), D2-EGFP (Gong et al., 2003) and the AI9 reporter mice (Madisen et al., 2010) were previously described. All lines were maintained by backcrossing to C57Bl/6J. All other experiments were conducted on 4-12 week old male C57/Bl6 micefrom Jackson Labs. Mice were weaned at ~21 days of age and housed in groups of 2-5 on a 12-hour light/dark cycle (lights on 0700-1900h), with free access to food and water except during behavioral testing. All procedures conformed to National Institutes of Health *Guidelines for the Care and Use of Laboratory Animals* and were approved by the Stanford University Administrative Panel on Laboratory Animal Care.

Behavioral Sensitization

All mice were given one day of saline injection for habituation. Subsequently, cocaine-treated mice received 5 consecutive days of 20 mg/kg cocaine (Sigma) while controls received 5 days of saline. Activity was monitored as previously described (Rothwell et al., 2014) in an arena (ENV-510, Med Associates) housed within a sound-attenuating chamber, equipped with a ventilation fan and illuminated by a single overhead light. The location of the mouse within the arena was monitored in three dimensions by arrays of infrared beams connected to a computer running Activity Monitor software (Med Associates). This software package calculated the distance travelled during 5-minute epochs, which were summed together to calculate total distance travelled throughout the entire 20-minute test session.

Virus Generation and In Vivo Stereotactic Injection

Rabies viruses were generated as previously described (Lim et al., 2012). In brief, HEK cells were transiently transfected with helper plasmids and SPBN

construct, and supernatant was transferred to BHK-B19G cells after 3 days. Following two amplification steps, benzonase-treated supernatant was filtered through a 0.22 μm filter, centrifuged at 20,000 RPM for 2 hr at 4ºC and resuspended in Opti-MEM (Life Technologies). Intracranial injection of virus in vivo was performed using a stereotaxic instrument (David Kopf) under general ketamine-medetomidine anesthesia. A small volume (750nl-1μL) of concentrated rabies virus solution was injected bilaterally into NAc (AP +1.50, ML +/-1.10, DV –4.40) or PVN of the hypothalamus (AP -0.60, ML +/-0.25, DV –5.40) at a slow rate (125nL per min) using a syringe pump (Harvard Apparatus). The injection needle was withdrawn 5 min after the end of the infusion. Mice were sacrificed 3-5 days after injection to minimize the effect of rabies virus infection on cellular transcription. For D1-MSN specific RV targeting, D1-Cre transgenic mice were first injected in the NAc with two mixed adeno-associated viruses: (1) AAV-hSynapsin-DIO-TVA and (2) AAV-hSynapsin-DIO-Rabies Virus Glycoprotein. One week was allowed for robust expression of both Cre-dependent viruses and a second injection was made into the NAc of rabies virus-EGFP, which had been pseudotyped with the EnvA coat protein. Injection of pseudotyped rabies virus in the absence of TVA expression did not label significant numbers of neurons. All AAVs were of the DJ-subtype and were generated by the Stanford University Viral Core.

Tissue mRNA isolation

For mRNA isolation, acute brain slices were prepared as per standard protocols and allowed to recover for 1.5 hours at RT. Tissue was micro-dissected from acute slices and mRNA was isolated with TRIzol reagent (Invitrogen, Carlsbad, CA.). To reduce between-subject variability, single cell experiments were designed as two-way comparisons of neuronal populations that could be isolated from the same animal. Pipette tips for cellular aspiration were backfilled with 0.5ul of 2X Cells Direct buffer (Cells Direct One-Step qRT-PCR kit, Invitrogen, Carlsbad, CA) and cytosolic contents were deposited in 0.5 μl RNase/DNase free PCR tubes containing 5ul of 2x buffer. Reverse transcription and 18 cycles of target specific PCR amplification was performed within the same tube, after

which 4 µl of ExoSAP-IT (Affymetrix, Cleveland, OH) was added to degrade remaining primers. Amplified libraries were loaded onto Fluidigm 96.96 microfluidics chips as per manufacturer's protocols (Fluidigm, South San Francisco, CA).

Single Cell Transcriptional Regulation

To assay single-cell coordination of individual splice sites, we focused on normalized expression data for ss4 of Nrxn1 and used the following equation

$$Nrxn1ss4\ Index = \frac{(E^{ss4in} - E^{ss4out})}{(E^{ss4in} + E^{ss4out})}$$

(where E = normalized expression) to generate a Nrxn1 ss4 splicing index. This index ranged from -1 (only Nrxn1 ss4-out) to +1 (only Nrxn1 ss4-in), with 0 representing a 1:1 ratio of expression in a single cell. Histograms were generated with the following arbitrary ss-index cutoffs: ss4-in (0.33→1), both(-0.33→0.33) and ss4-out (-0.33→-1).

SUPPLEMENTAL REFERENCES

Gong, S., Zheng, C., Doughty, M.L., Losos, K., Didkovsky, N., Schambra, U.B., Nowak, N.J., Joyner, A., Leblanc, G., Hatten, M.E., and Heintz, N. (2003). A gene expression atlas of the central nervous system based on bacterial artificial chromosomes. Nature *425*, 917-925.

Gong, S., Doughty, M., Harbaugh, C.R., Cummins, A., Hatten, M.E., Heintz, N., and Gerfen, C.R. (2007) Targeting Cre recombinase to specific neuron populations with bacterial artificial chromosome constructs. Journal of Neuroscience *27(37)*, 9817-9823.

Hippenmeyer, S., Huber, R.M., Ladle, D.R., Murphy, K., and Arber, S. (2007). ETS transcription factor Erm controls subsynaptic gene expression in skeletal muscles. Neuron *55*, 726-740.

Lim, B.K., Huang, K.W., Grueter, B.A., Rothwell, P.E., and Malenka, R.C. (2012). Anhedonia requires MC4R-mediated synaptic adaptations in nucleus accumbens. Nature *487*, 183-189.

Madisen, L., Zwingman, T.A., Sunkin, S.M., Oh, S.W., Zariwala, H.A., Gu, H., Ng, L.L., Palmiter, R.D., Hawrylycz, M.J., Jones, A.R.*, et al.* (2010). A robust and high-throughput Cre reporting and characterization system for the whole mouse brain. Nature Neuroscience *13*, 133-140.

Rothwell, P.E., Fuccillo, M.V., Maxeiner, S., Hayton, S.J., Gokce, O., Lim, B.K., Fowler, S.C., Malenka, R.C., and Südhof, T.C. (2014). Autism-associated neuroligin-3 mutations commonly impair striatal circuits to boost repetitive behaviors. Cell *158*, 198-212.

Shuen, J.A., Chen, M., Gloss, B., and Calakos, N. (2008). Drd1a-tdTomato BAC transgenic mice for simultaneous visualization of medium spiny neurons in the direct and indirect pathways of the basal ganglia. Journal of Neuroscience *28*, 2681-2685.